KfK 4958
November 1991

Current Lead and Bus Bar System for the 1.8 K Test of the EURATOM LCT-coil

G. Friesinger, R. Heller, L. Schappals, G. Zahn
Institut für Technische Physik
Projekt Kernfusion

Kernforschungszentrum Karlsruhe

KERNFORSCHUNGSZENTRUM KARLSRUHE

INSTITUT FÜR TECHNISCHE PHYSIK

Projekt Kernfusion

KfK 4958

CURRENT LEAD AND BUS BAR SYSTEM FOR THE 1.8 K TEST OF THE EURATOM LCT-COIL

G. Friesinger, R. Heller, L. Schappals, G. Zahn

Kernforschungszentrum Karlsruhe GmbH, Karlsruhe

Als Manuskript gedruckt

Kernforschungszentrum Karlsruhe GmbH
Postfach 3640, 7500 Karlsruhe 1

ISSN 0303-4003

Stromzuführungs- und Bussystem für den 1.8 K Test der EURATOM LCT-Spule

Zusammenfassung

Für den Test der EURATOM LCT-Spule bei 1.8 K in der TOSKA-Anlage ist der Einsatz der 23 kA Stromzuführungen vorgesehen, die für den Test der POLO Modellspule entwickelt werden. Besonderes Gewicht wird auf die Verbindung der Stromzuführungen zur Spule gelegt. Erstere werden durch überkritisches Helium bei 4.2 K gekühlt, während sich die Spulenwicklung auf einer Temperatur von 1.8 K befindet. Der Wärmestrom je Anschlußpol, der dadurch entsteht, bewegt sich in einem Bereich von 10 bis 15 W. Die Rechnungen zeigen, daß das System aus Stromzuführungen und supraleitendem Bus sicher ausgelegt ist; es widersteht einem Kühlmittelverlust für mehr als eine Minute mit nur sehr geringer Erhöhung der Wärmelast, wobei vorausgesetzt wurde, daß der Kühlkreis der Spulenwicklung weiter gekühlt wird.

Abstract

For the test of EURATOM LCT coil at 1.8 K in the TOSKA facility, it is foreseen to use the 23 kA current leads developed for the POLO model coil. Special emphasis has been given to the connection of the current leads which will operate by using supercritical helium at 4.2 K to the coil terminals which are on the 1.8 K level. The heat input from the bus bar system (4.2 K) to the coil winding cooling circuit (1.8 K) for each terminal is only in the range of 10 to 15 W. The calculations show that the current leads together with the superconducting connection bars are safe: They can withstand a loss of mass flow for more than one minute withonly a very small increase of heat load into the coil if its cooling circuit stays in operation.

Table of Contents

List of Illustrations

List of Tables

1. Introduction

As a special task within the European Fusion Technology Programme, it is foreseen to test the EURATOM LCT coil at 1.8 K in the TOSKA-Upgrade facility [1],[2]. For this purpose, current leads for currents up to 23 kA are needed. It was decided to use two of the leads presently under construction for the test of the POLO model coil and designed for a current region of 15 to 30 kA [3]. Figure 1 shows a scheme of the POLO current lead whereas in Table 1 the main parameters are summarized. The radial temperature dependence of the cooling ribs is factorized in a so-called "rib efficiency"-factor which has been calculated analytically [5].

Parameter	Unit	Value
Nominal current	kA	22
Current region	kA	0 - 30
Overall length	m	2.32
Bottom temperature of conductor $T_{Cu,bottom}$	K	4.5
Inlet temperature of helium $T_{He,bottom}$	K	4.5
Top temperature of conductor $T_{Cu,top}$	K	293
Outlet temperature of helium $T_{He,top}$	K	variable
Inlet pressure of helium	bar	4
RRR of conductor		6
Heat exchanger length l_{hex}	m	1.90
Length of superconducting part $l_{cold,1}$ (appendix)	m	0.15
Length of superconducting part $l_{cold,2}$ for length adjustment at different currents	m	0.95
Cross section of conductor A_{Cu}	cm^2	38.5
Cooled perimeter of heat exchanger P_{cool}	m	11.6
Cross section of helium A_{He}	cm^2	36.5
Inner diameter of cooling disks	mm	70
Outer diameter of cooling disks	mm	135.7
Transversal distance of cooling disks	mm	2
Disk thickness	mm	1
Hole diameter in cooling disks	mm	1.6
Minimum hole distance in cooling disks	mm	2.5
RRR of cooling disks		6
Rib efficiency of cooling disks		function of temperature

Table 1. General input parameters for the calculations of the POLO current lead

Therefore is was decided to calculate the behaviour of the current lead in connection with the superconducting bus bar to the LCT coil by means of the computer code CURLEAD [4].

Three different operating conditions have been investigated.

- Stand-by operation i.e. zero current
- Steady state operation at 17 kA and 23 kA
- Emergency situations i.e. loss of mass flow and
  - safety discharge of the LCT coil, resp.
  - no discharge of the coil.

The cooling scheme of the superconducting bus bar as well as the geometrical dimensions with respect to stability against loss of mass flow is studied, too.

One special attention was given to the cooling behaviour of the coil terminals because of the change of the operating temperature from 3.5 K to 1.8 K whereas the superconducting bus bars resp. the current leads are not cooled by evaporating liquid helium anymore but by supercritical helium at 4.2 K and about 4 bar. The amount of heat resulting from conduction due to the temperature difference at the coil terminal of $\Delta T = 4.2 - 1.8\ K = 2.4\ K$ has to be known. In addition, a thermal short circuit has to be prevented.

Some calculations concerning the change of mass flow rate and the response of the current lead and bus system have been also done.

Finally, the maximum temperature in the superconducting bus has been computed which will be reached during a energy dump of the LCT coil due to eddy currents generated by the magnetic field change.

In the following, the final design will be given, and the computational results are presented. Figure 2 shows a scheme of the coil-lead-system including the superconducting bus bar and its connections to the coil terminal resp. the current lead. This system will be installed in horizontal position within the vacuum vessel.

In the next section, the design of the current lead and bus system will be described.

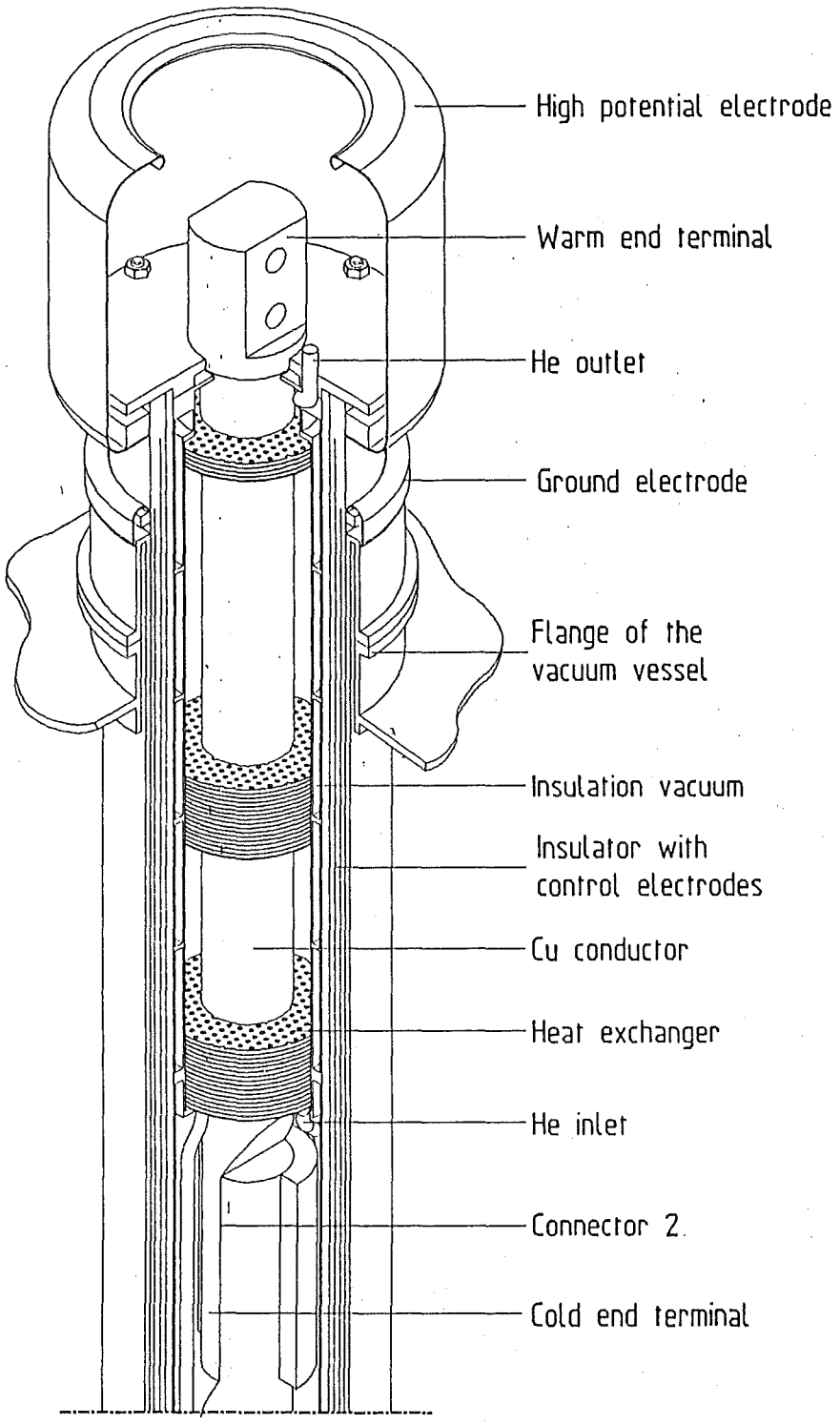

Figure 1. Longitudinal cross section of the current lead: The heat exchanger is shown as well as the cold and warm end connections

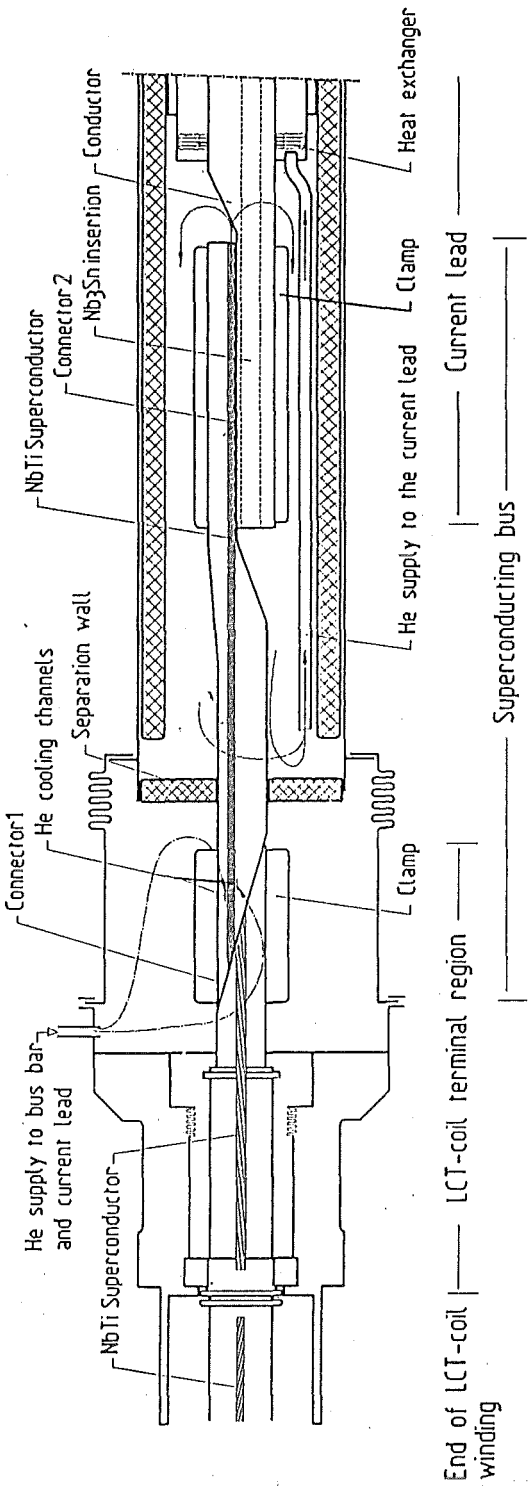

Figure 2. Scheme of the LCT coil current lead connection: The superconducting bus and its connections to the coil terminal and the cold end of the lead is included in the figure. The system will be installed in horizontal position within the vacuum vessel

2. Design of the current lead and bus bar system

2.1 General remarks

The current lead and bus bar system consists of three regions i.e.

- the LCT-coil terminal,
- the superconducting bus,
- the current lead,

connected by two joints. The scheme is shown in Figure 2.

The current lead and bus bar system is designed for the following requirements:

1. maximum operation current : 23 kA
2. maximum operation voltage : 2.5 kV
3. Test voltage : 10 kV
4. Operating temperature : 4.2 K
5. Operation without active cooling (LCT-coil winding will be cooled) : at least 1 min without quench

In the following, the three regions including their connectors are described in detail.

2.2 LCT-coil terminal region

The existing LCT-coil terminal as shown later on in Figure 4 was originally designed for 11.4 kA and was bath-cooled at 4.5 K. The coil winding was cooled by supercritical helium at 3.5 K, and the current lead side was bath-cooled at 4.5 K.

To maintain the operation current of 23 kA, the winding pack has to be cooled with 1.8 K supercritical helium, and the current lead and bus system will be cooled with 4.2 K supercritical helium.

As will be described in section 3., the calculations show that it is not necessary to cool the coil terminal actively with helium but only by conduction. This eases the design of the bus bar system because no change of the existing terminal is required.

2.3 Superconducting bus bar region and connectors

The superconducting bus bar system consists of a short length of the LCT superconductor whose steel jacket has been dismantled. The LCT superconductor will be soft soldered in a copper bar for electrical and mechanical stabilization. The cross section of the bus bar is shown in Figure 3 whereas the geometrical numbers are summarized in Table 2.

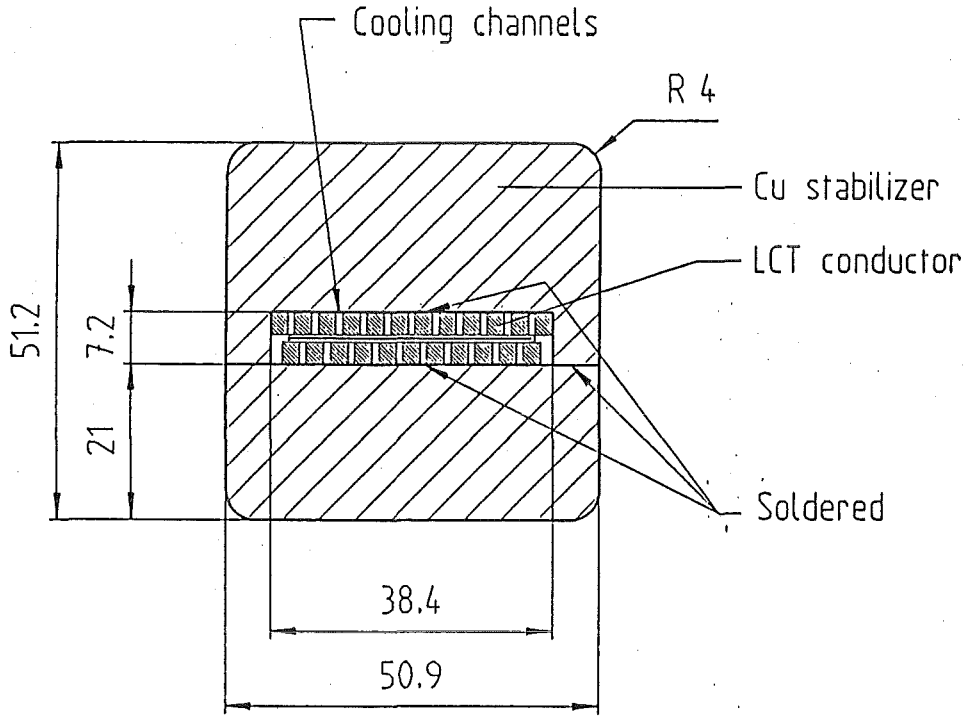

Figure 3. Cross section of the superconducting bus bar

Parameter	Unit	Value
Length of s.c. bus	m	0.51
RRR of copper of s.c. bus		50
ρ(T=4.2K,B=0.6T,RRR=50)	Ωm	$2\ 10^{-10}$
Outer dimensions of the LCT conductor axial x radial (dismantled)	mm x mm	38.4 x 7.2
Cross section of LCT conductor A_{LCT} (dismantled)	cm^2	2.7648
Cross section of copper in LCT conductor $A_{Cu\text{-}LCT}$	cm^2	1.38
Cross section of NbTi in LCT conductor $A_{NbTi\text{-}LCT}$	cm^2	0.29
Cross section of helium in LCT conductor $A_{He\text{-}LCT}$	cm^2	0.95
Cooled perimeter of strands P_{cool}	cm	16.5
Outer dimensions of the s.c. bus axial x radial	mm x mm	50.9 x 51.2
Cross section of copper profile of the s.c. bus $A_{Cu\text{-}prf}$	cm^2	21.32

Table 2. General data of the superconducting bus bar

The whole connection area is enclosed in steel pipes and a bellow.

The superconducting bus bar will be cooled by supercritical helium at 4.2 K and 4 bar. The helium enters the connector 1 region on the left side, filling this region, and flowing through the cooling channels inside the LCT superconductor. The helium enters the LCT conductor through cooling channel which are milled in the clamps and the stabilizing copper bar of the connector 1. It exits the LCT conductor at the end of connector 2.

To get a counterflow around the connector 2 and outside the superconducting bus bar, the connector area is divided by a separation wall as shown in Figure 2. In addition, the inlet pipe of the current lead heat exchanger will be extended near to this wall. The helium flow is indicated in the figure, too.

The shape of the connector 1 was determined by the LCT specifications. In order to provide a sufficient contact pressure to obtain an electrical resistance of $10^{-8}\Omega$, clamps will be used as shown in Figure 3. They will be bolted together.

The connector 2 is designed as single-lap-joint. The contact area will be larger than in connector 1 in order to reduce the electrical resistance. For the same reason, the distance between the connecting surface and the LCT superconductor will be only 2 mm.

2.4 Current lead region

The design of the current lead itself is described elsewhere [3].

3. Cooling behaviour of the coil bus bar connection

First, the heat load of the coil terminal has been investigated.

As already mentioned, the coil winding of the EURATOM LCT coil will be operated at 1.8 K whereas the superconducting bus bars resp. the current leads will be cooled by 4.2 K supercritical helium. Originally, a liquid helium bath was located around the coil terminal and around the bus bars up to the cold end of the current leads.

The question was wether it will be necessary to cool the coil terminals with supercritical helium in order to reduce the thermal heat load onto the coil winding or not. Additional cooling would complicate the design.

Figure 4 shows the cross section through the coil terminal.

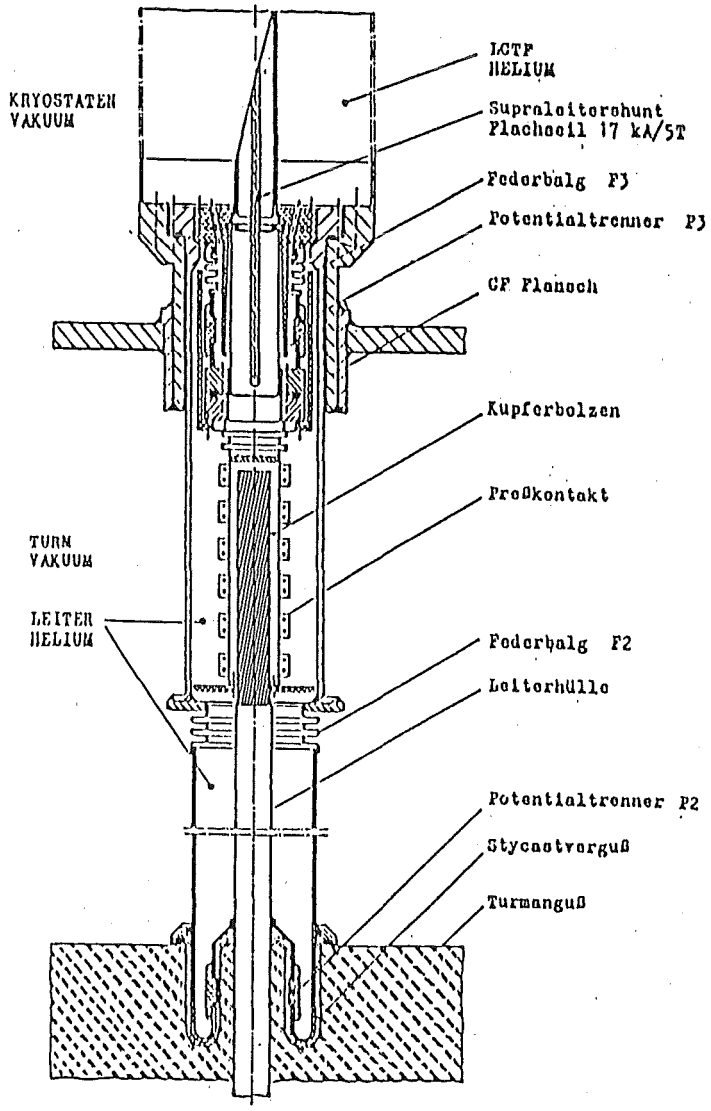

Figure 4. Longitudinal cross section of the coil terminal: The drawing is given in [6]

To study the effect of different cooling configurations at the coil terminal, the temperature distribution as well as the heat losses were computed by modeling the coil terminal together with the connector and the superconducting bus bar. There, an RRR of the copper of 50 was assumed.

After modeling the geometrical configuration, the heat load has been calculated by varying the cooling scheme of the connection part i.e. the distance of the inlet of the cooling of the connector to the outlet of the coil winding, $d_{uncooled}$. First the temperature of the end of the winding was fixed to 1.8 K, and the inlet temperature of the helium of the connector to 4.2 K. In a second step, the temperature at the end of the winding was varied between 1.8 K and 2.4 K for a fixed distance $d_{uncooled}$. The thermal conductivity of the copper below 4.2 K was extrapolated by using the Wiedemann-Franz law. (see Figure 5).

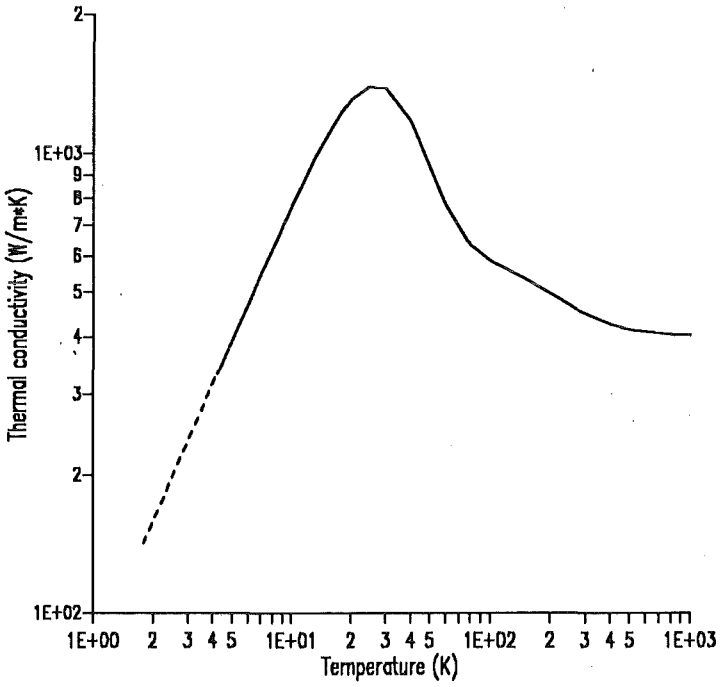

Figure 5. Thermal conductivity vs temperature for high conductivity copper: The numbers are computed by using a modified relation of the Wiedemann-Franz law as used in [4]. The full line denotes the values beyond 4.2 K which are verified whereas the dashed line denotes the values extrapolated down to 1.8 K. A residual resistivity ratio of 50 was used

Figure 6 shows the temperature of the copper as a function of position for different $d_{uncooled}$, whereas at the top of Figure 6 the connection to the superconducting bus bar is shown. Figure 7 shows the heat load towards the coil winding vs $d_{uncooled}$. All calculations were done for a current of 23 kA which is more than the critical current of the LCT conductor of roughly 20 kA at 1.8 K and 11 T. If the outlet temperature of the coil winding will be higher, the corresponding heat load will decrease due to the smaller temperature gradient.

It can be clearly seen that it is not recommended to cool the coil terminal itself because the difference between the heat loads for small and large $d_{uncooled}$ is only 5 %. Therefore, it was decided to fix the inlet of the cooling for the bus bar and the current lead system at the end of the coil terminal i.e. for the following calculations, $d_{uncooled}$ was set to 32 cm.

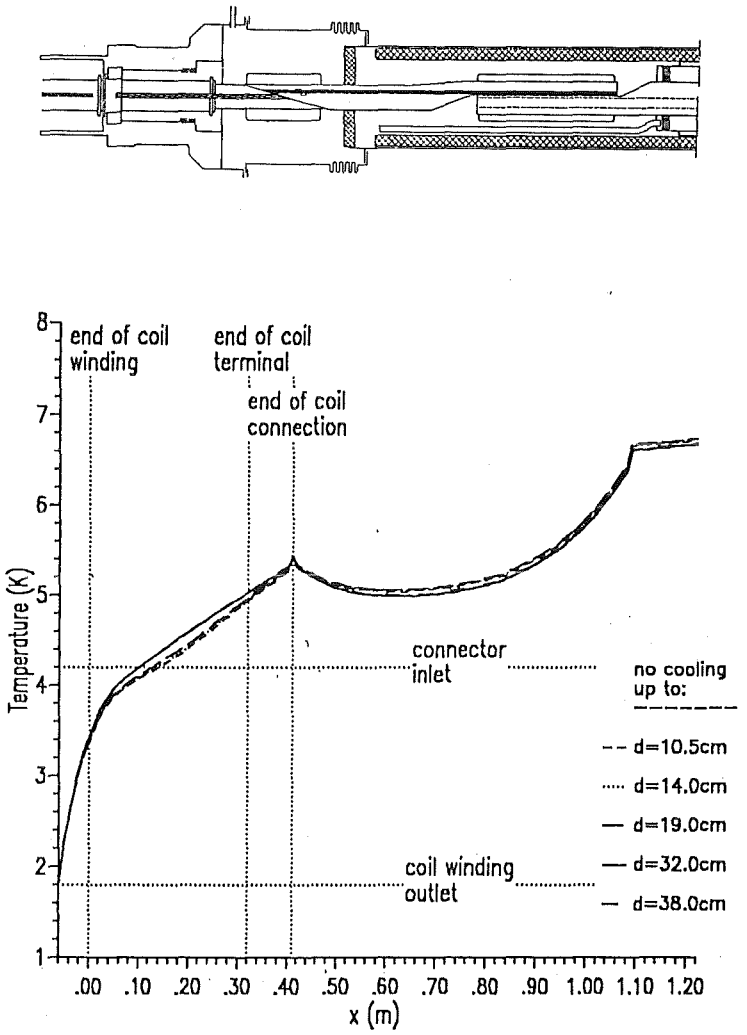

Figure 6. **Cross section through the coil terminal including the connector and copper temperature vs longitudinal position:** On the top, a longitudinal cross section through the coil terminal including the connector to the superconducting bus bar is shown. At the bottom, the copper temperature as a function of the longitudinal position is plotted for different uncooled lengths, $d_{uncooled}$

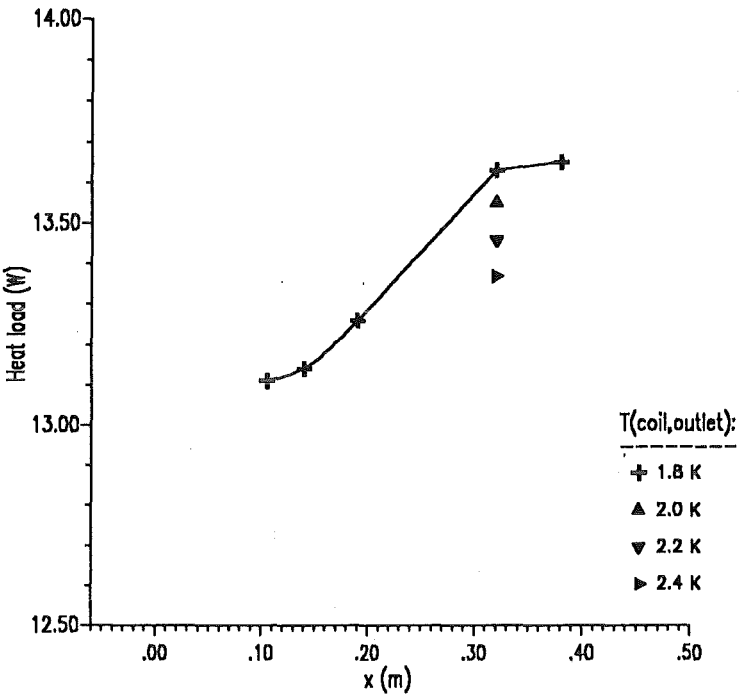

Figure 7. Heat load vs the distance of the helium inlet of the connector to the coil winding outlet: The different symbols denote different outlet temperatures of the coil winding

4. Calculation results of the current lead and bus bar system

4.1 General remarks

In the first approach, the current leads were positioned vertically at the outside of the TOSKA vacuum vessel. This results in a rather long superconducting bus bar which had to be bended at its end by 90 degrees.

Due to the fact that the leads will be cooled by supercritical helium, i.e. no liquid helium bath is needed, it was decided to change the design. Now the current leads are positioned horizontally which results in a rather short bus bar. This current lead and bus bar system has been described in section 2.

The resulting question was the safety behaviour of the current lead and bus system with respect to a loss of helium mass flow.

But at first, the optimum mass flow rate and the resulting temperature profile have been calculated for different operating currents i.e. between 0 and 30 kA. The results have been compared to the numbers from computations done without a superconducting bus i.e. fixed copper and helium temperatures at the bottom end of the heat exchanger.

As already mentioned, the main parameters of the POLO current lead has been summarized in Table 1. The operation parameters of the lead-bus-system are summarized in Table 3.

Parameter	Unit	Value
Nominal current	kA	18
Current region	kA	0 - 23
Length of the bus bar (incl. coil terminal)	m	1.22
Length of current lead	m	2.28
Bottom temperature of conductor $T_{Cu,bottom}$	K	1.8
Inlet temperature of helium $T_{He,bottom}$	K	4.2
Inlet pressure of helium	bar	4
Top temperature of conductor $T_{Cu,top}$	K	293
Outlet temperature of helium $T_{He,top}$	K	variable
RRR of conductor of bus		50
RRR of conductor of lead		6

Table 3. Operational parameters of the lead and bus bar system

4.2 Steady state operation

The optimum mass flow rate as well as the temperature profile has been computed for various operating currents.

The optimum mass flow rate was obtained by varying the mass flow rate for each current until the heat load out of the cold end was below 1 W.

Figure 8 shows the temperature profiles of the POLO current lead for zero current, 17, 23, and 30 kA with the lower end of the heat exchanger fixed to 4.5 K. Table 4 shows the main results of the

calculations. The mass flow rates given below are not the completely optimized ones. Therefore the resultant quantities like voltage drop, pressure drop, and temperatures at the warm end of the current lead show no clear dependence on the mass flow rate used. The reason is the large sensitivity of the temperature profile to changes in mass flow due to the long superconducting part of the current lead heat exchanger. This will be discussed in detail at the end of this section. The temperature at the upper end of the superconducting part decreases with increasing current due to the fact that the superconducting length increases. The zero current case shows another profile and can not be related to the current cases 17 kA, 23 kA, and 30 kA.

I	$\dot{m}$	ΔU	Δp	Q_{bottom}	T_{cold}	$T_{max,Cu}$	$T_{top,He}$
[kA]	$[\frac{g}{s}]$	[mV]	[mbar]	[W]	[K]	[K]	[K]
0	0.380	0.00	0.21	0.26	69.18	293.0	249.6
17	0.913	76.63	0.71	0.00	81.04	293.0	279.1
23	1.250	73.86	0.72	0.00	21.27	293.0	267.0
30	1.680	102.12	1.15	0.00	9.28	306.6	297.7

Table 4. Main results of the load line calculations for the POLO current lead without superconducting bus bar: T_{cold} denotes the temperature at the upper end of the superconducting part of the current lead

Afterwards, the superconducting bus bar as well as the different connections were modelled. The bottom end of the modelled conductor represents the end of the coil winding and was therefore fixed to 1.8 K. The inlet of the helium cooling to the bus bar and the lead was set to $d_{uncooled} = 32$ cm i.e. at the end of the coil terminal.

Then the calculations done for the current lead were repeated for the whole arrangement. Starting from the optimum mass flow rate obtained for the case without bus bar system, the mass flow rates were changed until the maximum temperature at the warm end of the current lead was in the range of 293 to 300 K. Table 5 summarizes the results, and the temperature profiles are plotted in Figure 9.

The difference in the bottom heat load is due to the temperature gradient between the 1.8 K level of the coil winding and the 4.2 K level of the superconducting bus bar cooling.

I	$\dot{m}$	ΔU	Δp	Q_{bottom}	T_{cold}	$T_{max,Cu}$	$T_{top,He}$
[kA]	$[\frac{g}{s}]$	[mV]	[mbar]	[W]	[K]	[K]	[K]
0	0.380	0.00	0.25	1.02	68.61	293.0	249.5
17	0.922	76.48	0.74	8.25	79.32	293.0	277.5
23	1.270	79.42	0.87	13.61	30.27	293.0	272.1
30	1.800	92.62	1.17	21.62	9.93	295.4	273.0

Table 5. Main results of the load line calculations for the POLO current lead with superconducting bus bar: T_{cold} denotes the temperature at the upper end of the superconducting part of the current lead

In Figure 10 the mass flow rate is plotted vs the operating current. It can be clearly seen that at lower currents the lead is too short i.e. the mass flow rate will be higher than the optimum one to balance the heat load. At higher currents, the current lead is too long i.e. the mass flow rate will be higher than the optimum one to prevent overheating. In between, the range of optimum current is rather large due to the use of the Nb_3Sn insertion over a length of 1.1 m which serves as an

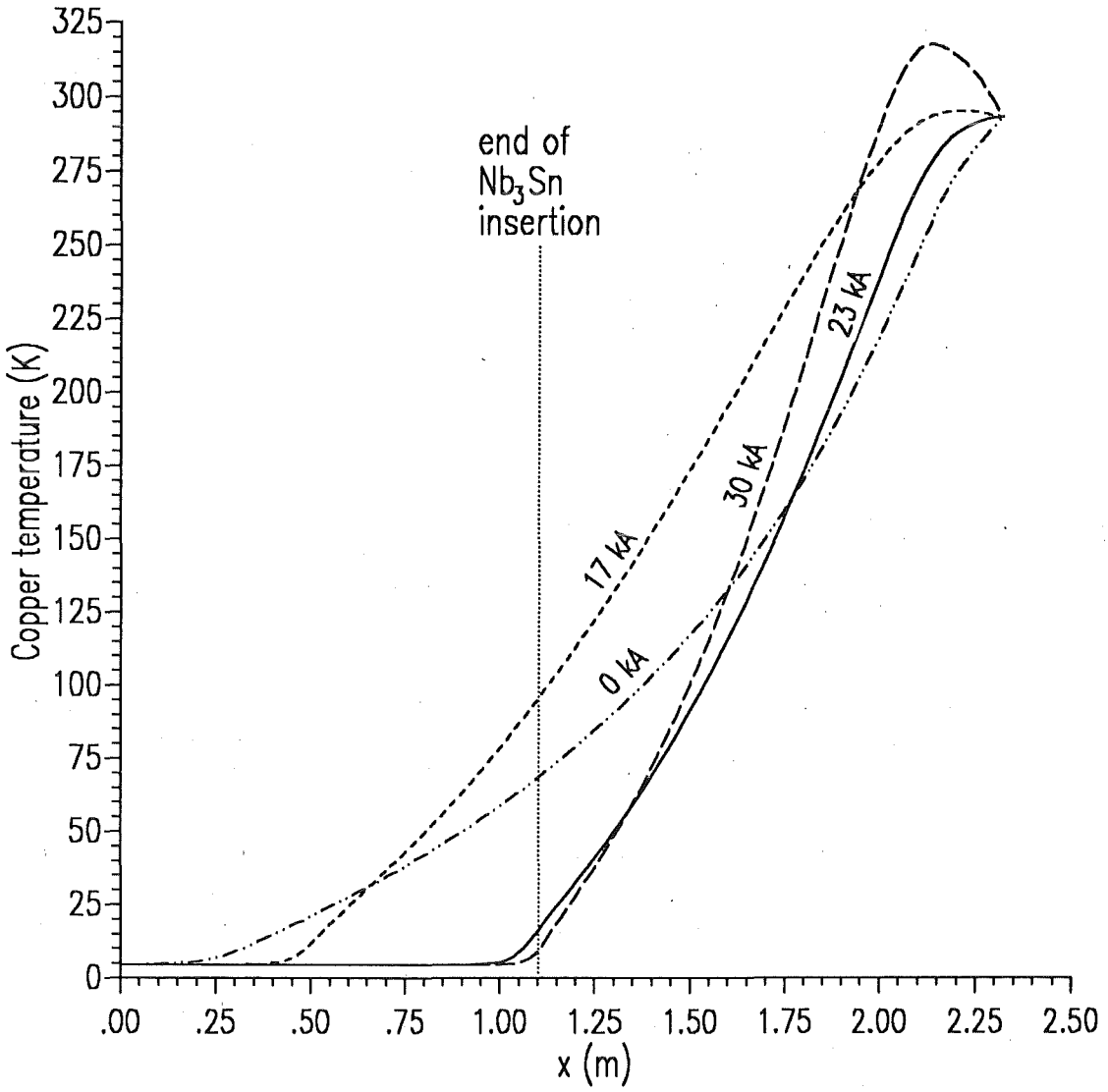

Figure 8. Temperature profiles of the POLO current lead for 0,17, 23, and 30 kA without superconducting bus bar: The optimum mass flow rates are for 0 kA 0.38 g/s, for 17 kA 0.915 g/s, for 23 kA 1.25 g/s, and for 30 kA 1.67 g/s

automatic adjustment of the normal conducting length. It is possible to **operate the lead with optimum mass flow not only for one current but for a range of currents**.

Figure 11 shows the heat load as a function of current. The full line corresponds to the heat load at the bottom end of the superconducting bus bar i.e. the load to the coil winding. The dashed line

denote the heat load from the current lead to the bus bar. The negative sign counts for the fact that for high currents, the Joule heating generated in the bus bar lead connector is large but the cooling capability of the current lead heat exchanger is able to transfer the heat to the helium i.e. the temperature at the cold end of the heat exchanger is lower than the one of the connector, the gradient is consequently negative. The heat load towards the coil winding is as large as calculated for the bus system itself i.e. there is no additional heat load originating from the lead which can be concluded also from the negative sign of the heat load at the cold end of the current lead heat exchanger. The heat load out of the cold end of the current lead without bus bar is plotted as full circles. If comparing this to the corresponding numbers with bus bar, it can be clearly seen that the mass flow rate in the case with the superconducting bus bar is a little too high for the lead itself.

The conclusion is that one has to optimize the current lead together with the superconducting bus bar system to get minimum losses .

It should be mentioned that the heat load at the cold end of the current lead heat exchanger depends strongly on the mass flow rate i.e. a slight change of $\dot{m}$ leads to a drastic change of the heat load if running near to the optimum mass flow rate. This can be seen in Figure 12 where the heat load towards the coil winding is plotted as a function of mass flow rate for 23 kA (solid line). The reason for this effect is the length of the superconducting part of the lead and bus system: if running near the optimum mass flow rate, a small reduction of the mass flow rate leads to a higher temperature and consequently to a drastic increase of the Joule heating at the region of the superconductor. Picturally spoken, a transition of a superconducting unit length Δx to a normal conducting state leads to an additional heat load to both neighbouring unit lengths and consequently to an increase of the temperature. The same happens for the next unit length towards the cold end which also was in a superconducting state etc. The longer the superconducting part of a current lead or the higher the operating current, the larger is the change of the amount of heat load. The heat load for higher mass flow rates doesn't drop to zero because of the temperature gradient from 4.2 K (bus bar system) to 1.8 K (coil winding) due to the thermal conductivity and the additional Joule heating in the copper part of the coil terminal.

Figure 12 shows also the heat load calculated for the heat exchanger i.e. without warm end and bus bar system. The differences in heat load compared to the calculations with bus bar system are twice i.e.

- for high mass flow rates:
  there is neither a temperature gradient nor a Joule heating in the superconducting part of the heat exchanger.
- for low mass flow rates:
  there is a smaller resistance due to the shorter superconducting length and therefore a smaller Joule heating in case of a normal conducting state resulting in a smaller heat load out of the cold end of the current lead.

In the following, the mass flow rate which corresponds to the particular step in heat load will be called **critical mass flow rate**.

We will return to this unbalanced effect later.

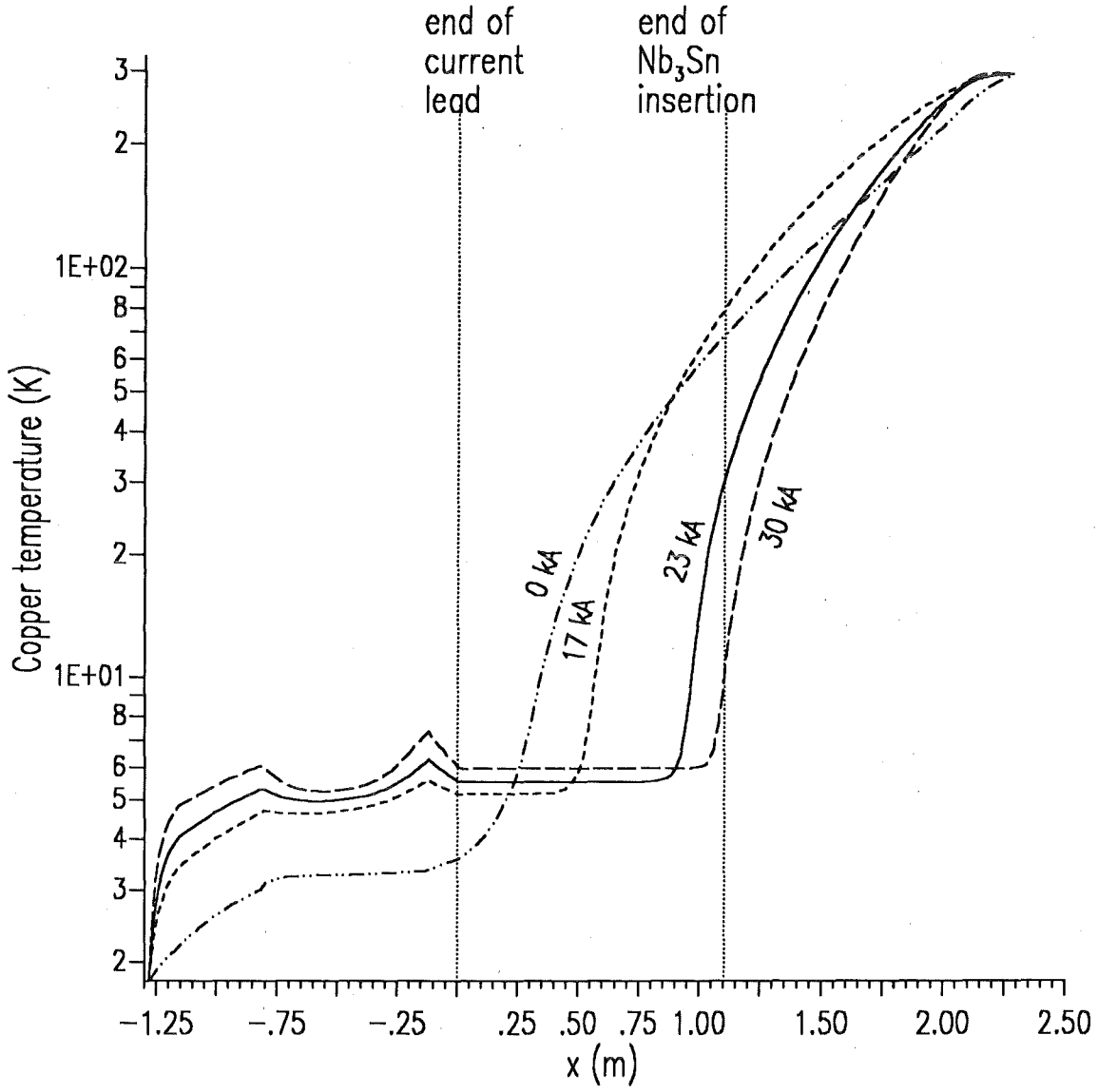

Figure 9. Temperature profiles of the POLO current lead for 0,17, 23, and 30 kA with superconducting bus bar: The optimum mass flow rates are for 0 kA 0.38 g/s, for 17 kA 0.922 g/s, for 23 kA 1.27 g/s, and for 30 kA 1.80 g/s The distributions are plotted on a logarithmic scale to see the effect of the lead-bus-connections

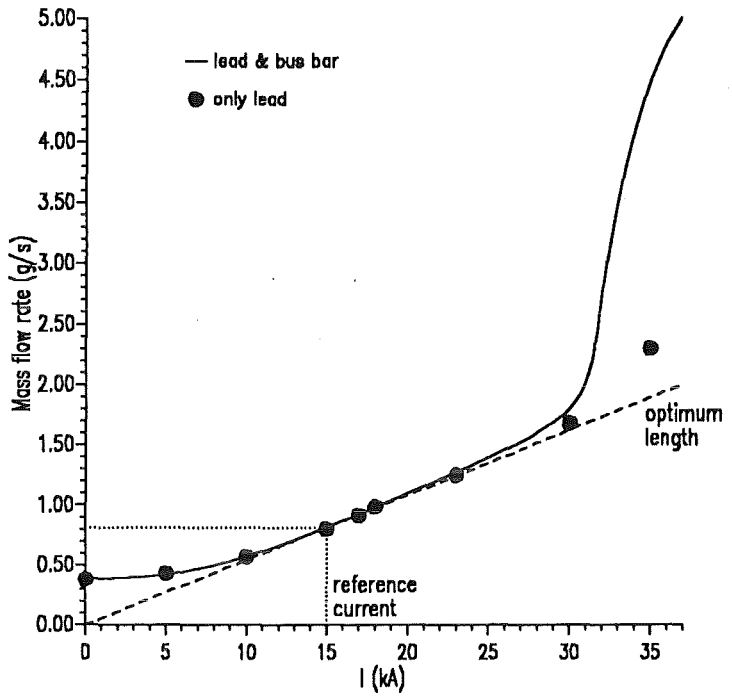

Figure 10. **Mass flow rate vs current of the lead-bus-system:** The dashed line corresponds to the optimum flow rate length correlation, the full circles denote the numbers of the current lead calculated without bus bar

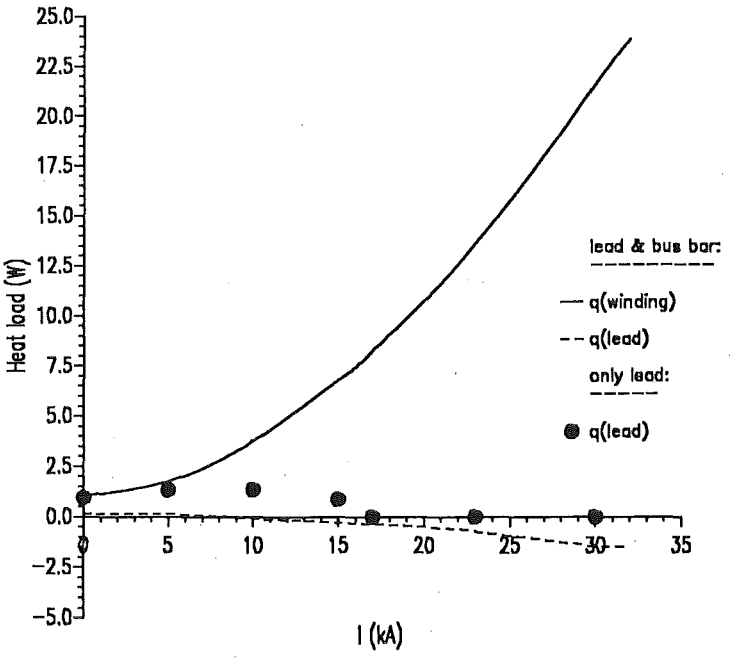

Figure 11. **Heat load vs current of the lead-bus-system:** The full line denotes the heat load at the end of the coil, the dashed line corresponds to the heat load at the bottom end of the current lead. The full circles represent the calculated numbers for the current lead calculated without bus bar

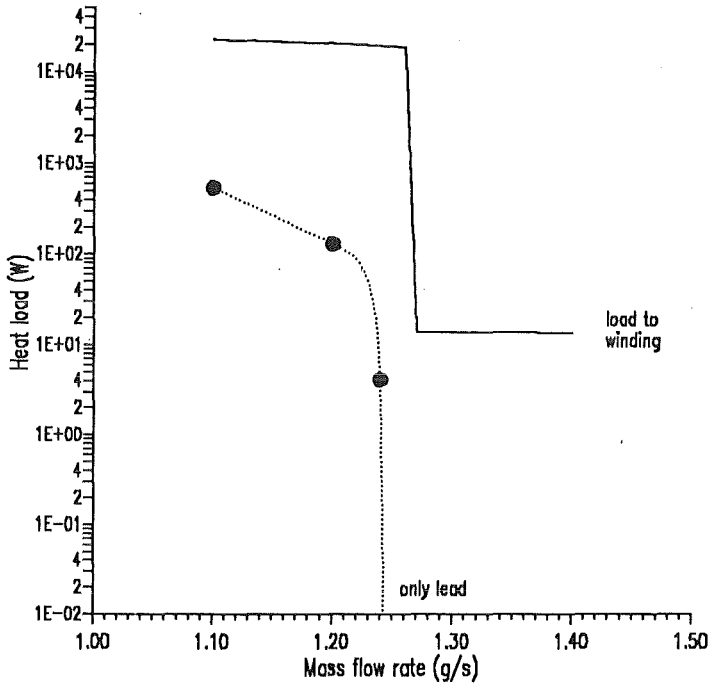

Figure 12. Heat load vs mass flow rate of the lead bus-system for 23 kA: The full line denotes the heat load from the bus bar to the coil winding, the full circles correspond to the heat load from the heat exchanger to the coil winding without bus bar system

4.3 *Loss of mass flow*

The effect of loss of helium mass flow was studied for the operational current of 23 kA. It was assumed that the cooling circuits of the LCT coil are continously operating.

The transient behaviour of the lead and bus system was computed by starting from the steady state solution for 23 kA. Then the mass flow was set to zero, and the temperature profiles as well as the heat load towards the coil winding has been computed for different time steps

- first by reducing the current exponentially with a dump time constant of $\tau = 15$ s,
- second by keeping the current at 23 kA.

The latter situation would occur if the two main switches of the power supply which are connected in series stay closed, and other actions have to be initiated.

The dump time constant was calculated by using the magnetic energy stored in the LCT coil, the current and maximum dump voltage i.e.

$$\tau = \frac{2\,Q}{I\,U_D} = \frac{L\,I}{U_D}$$

Using $I = 21$ kA, $L = 1.57$ H, and $U_D = 2.5$ kV, results in $\tau = 13$ s. In the following, $\tau = 15$ s will be used.

Figure 13 and Figure 14 show the temperature distributions which correspond to the two cases investigated. The heat load towards the coil winding as a function of time is plotted in Figure 15. The results are summarized in Table 6.

The conclusion is that the loss of mass flow with a consecutive dump of the LCT coil is no problem. If the energy dump is prevented, the heat load increases to about 60 W after 2 minutes whereas no overheating will occur.

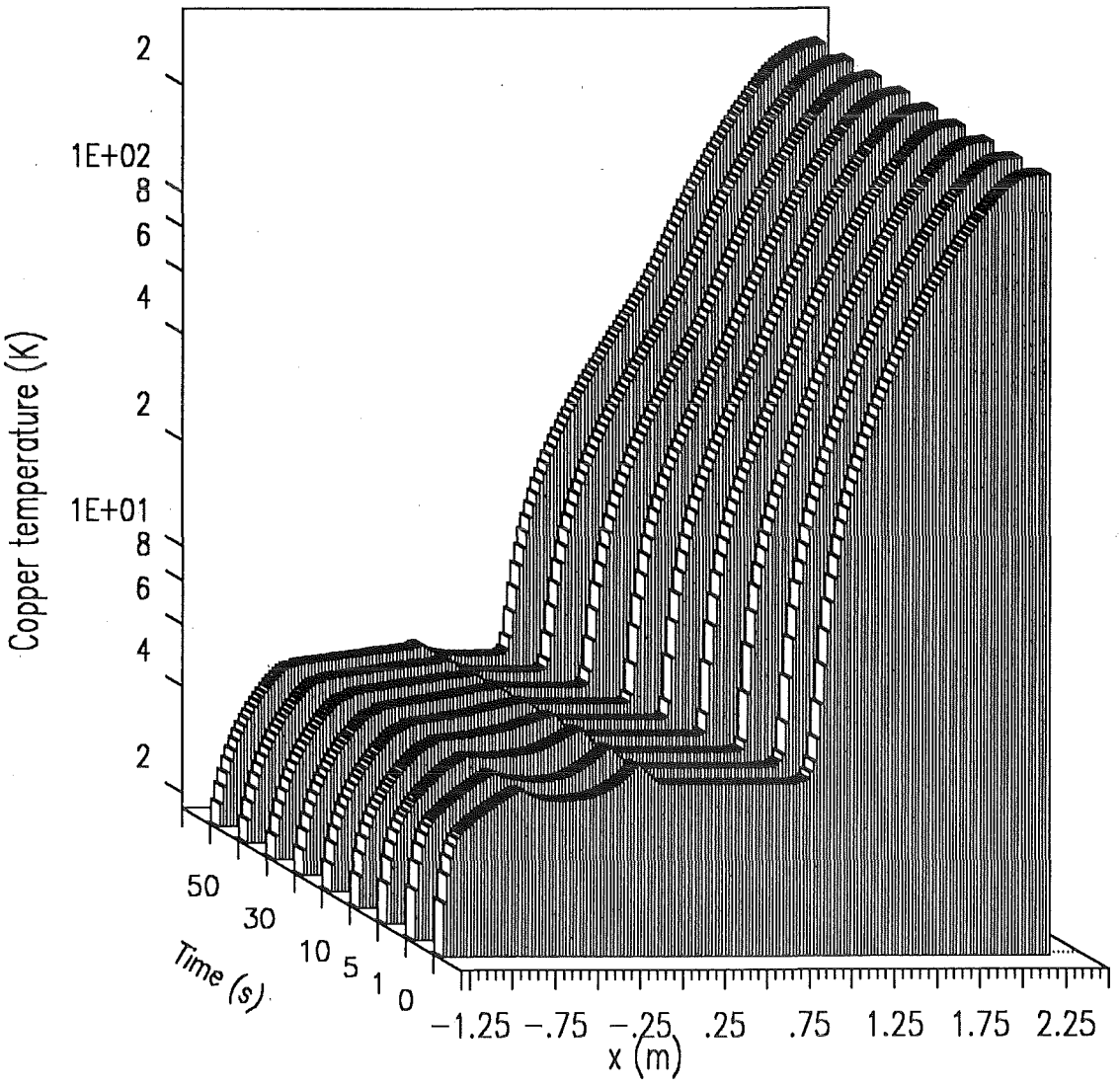

Figure 13. Temperature profiles of the lead bus system for 23 kA with energy dump: The profiles are shown at different times after switching off the mass flow

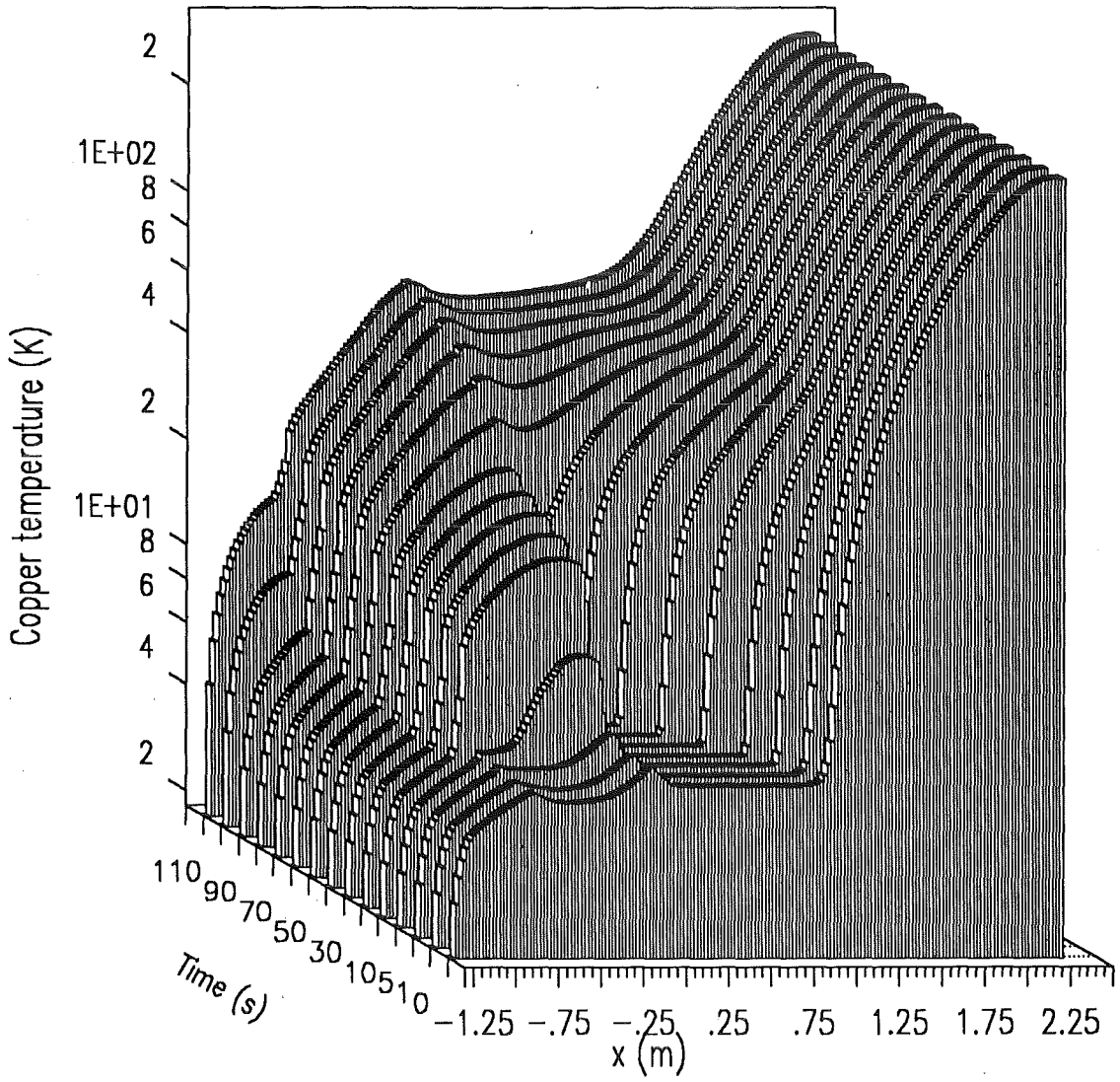

Figure 14. Temperature profiles of the lead bus system for 23 kA without energy dump: The profiles are shown at different times after switching off the mass flow

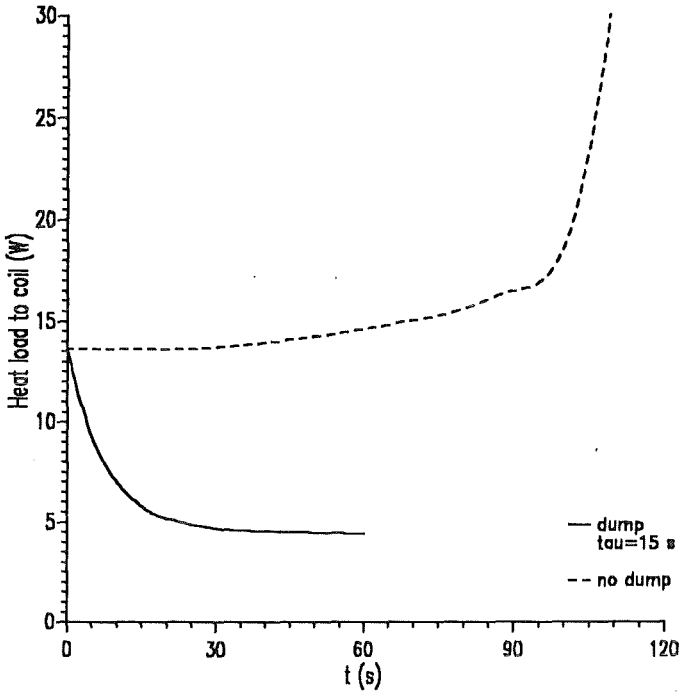

Figure 15. Heat load towards the coil winding vs time in case of loss of mass flow: The full line corresponds to the case with energy dump, the dashed line denotes the numbers in case of no energy dump

Time	$\dot{m}$	ΔU	Δp	Q_{bottom}	T_{cold}	$T_{max,Cu}$	$T_{top,He}$
[s]	$[\frac{g}{s}]$	[mV]	[mbar]	[W]	[K]	[K]	[K]
with energy dump							
0	1.270	79.42	0.87	13.61	30.27	293.0	272.1
1	0.0	74.83	0.0	12.51	31.74	293.0	288.14
5	0.0	58.42	0.0	9.24	35.88	293.0	288.07
10	0.0	42.56	0.0	6.98	38.84	293.0	287.66
15	0.0	30.89	0.0	5.80	40.75	293.0	287.14
20	0.0	22.38	0.0	5.19	42.17	293.0	286.59
30	0.0	11.71	0.0	4.69	44.28	293.0	285.52
40	0.0	6.11	0.0	4.54	45.92	293.0	284.56
50	0.0	3.18	0.0	4.47	47.29	293.0	283.73
60	0.0	1.66	0.0	4.42	48.47	293.0	282.99
without energy dump							
0	1.270	79.42	0.87	13.61	30.27	293.0	272.1
1	0.0	80.00	0.0	13.61	31.78	293.0	288.25
5	0.0	81.83	0.0	13.61	36.58	293.0	288.27
10	0.0	85.57	0.0	13.61	40.74	293.0	287.27
20	0.0	91.70	0.0	13.60	46.38	293.0	286.29
30	0.0	95.88	0.0	13.69	50.14	293.0	285.31
40	0.0	100.04	0.0	13.92	52.72	293.0	284.34
50	0.0	104.30	0.0	14.23	54.73	293.0	283.39
60	0.0	110.89	0.0	14.60	56.43	293.0	282.41
70	0.0	112.80	0.0	15.04	57.94	293.0	282.46
80	0.0	113.80	0.0	15.59	59.30	293.0	282.52
90	0.0	115.63	0.0	16.48	60.57	293.0	282.57
100	0.0	117.64	0.0	18.63	61.76	293.0	282.65
110	0.0	120.05	0.0	31.59	62.88	293.0	282.72
120	0.0	121.91	0.0	57.64	63.96	293.0	288.78

Table 6. **Main results of the transient calculations for the POLO current lead with superconducting bus bar with and without energy dump:** T_{cold} denotes the temperature at the upper end of the superconducting part of the current lead

4.4 *Remarks on mass flow control possibilites for the lead bus system*

4.4.1 Change of mass flow at 23 kA

The time scale of the strong dependence of the heat load at the cold end of the current lead heat exchanger on the mass flow rate has been studied. One wants to know how fast the current lead bus system reacts on a small change of the mass flow rate if operating near the critical mass flow rate (see Figure 12).

It results that this unbalanced effect happens on a large time scale due to the high thermal capacity of the lead bus system. This can be seen in Figure 16 where the temperature profile of the lead and bus bar system is plotted for different times after changing the mass flow rate from 1.30 g/s to 1.10 g/s. After 90 min (!), the temperature profile is only slightly changed, moreover, the profile of the bus bar system resp. the heat load to the coil winding didn't change during this time.

These results obtained by variing the mass flow rate of the current lead and bus system for 23 kA leads to the question which possibilites arise for mass flow control. Therefore, in Figure 17 the conductor temperatures at different positions i.e. at the cold end of the heat exchanger, at the connector region I resp. II, and at the end of the superconducting part $I_{cold,1}$ (so-called appendix) are plotted as a function of time. All these temperature levels react immediately after the change of the mass flow rate, but the value is only in the range of 0.08 K to 0.13 K for the time scale envisaged. After a long time i.e. more than four hours the temperatures start to increase again beginning from the position which is nearer to the warm end. The reason is that now overheating will start at the warm region of the current lead which conducts towards the cold end and furthermore leads to additional temperature increase due to Joule heating. **This means that the temperatures in the cold region of the lead and bus bar system are no good quantities for control.**

In Figure 18 and Figure 19, the voltage drop along the lead bus system and the temperatures at the top end of the heat exchanger resp. at the 80 per cent position in length are plotted as a function of time. These quantities vary strongly with time after changing the mass flow rate i.e. they are sensitive to it. **The temperature at the 80 per cent position in length inside the heat exchanger is the better quantity for control because of its independence on the operational current i.e. it is possible to use it also in case of zero current** . The POLO current leads are equipped with Pt 100 temperature sensors at this position.

It should be noted that the temperatures at the warm end as well as the voltage drop increase in this case because the steady state condition for a mass flow rate of 1.10 g/s leads to a completely overheating i.e. copper temperatures at the warm end of more than 1000 K resp. a voltage drop of several volts.

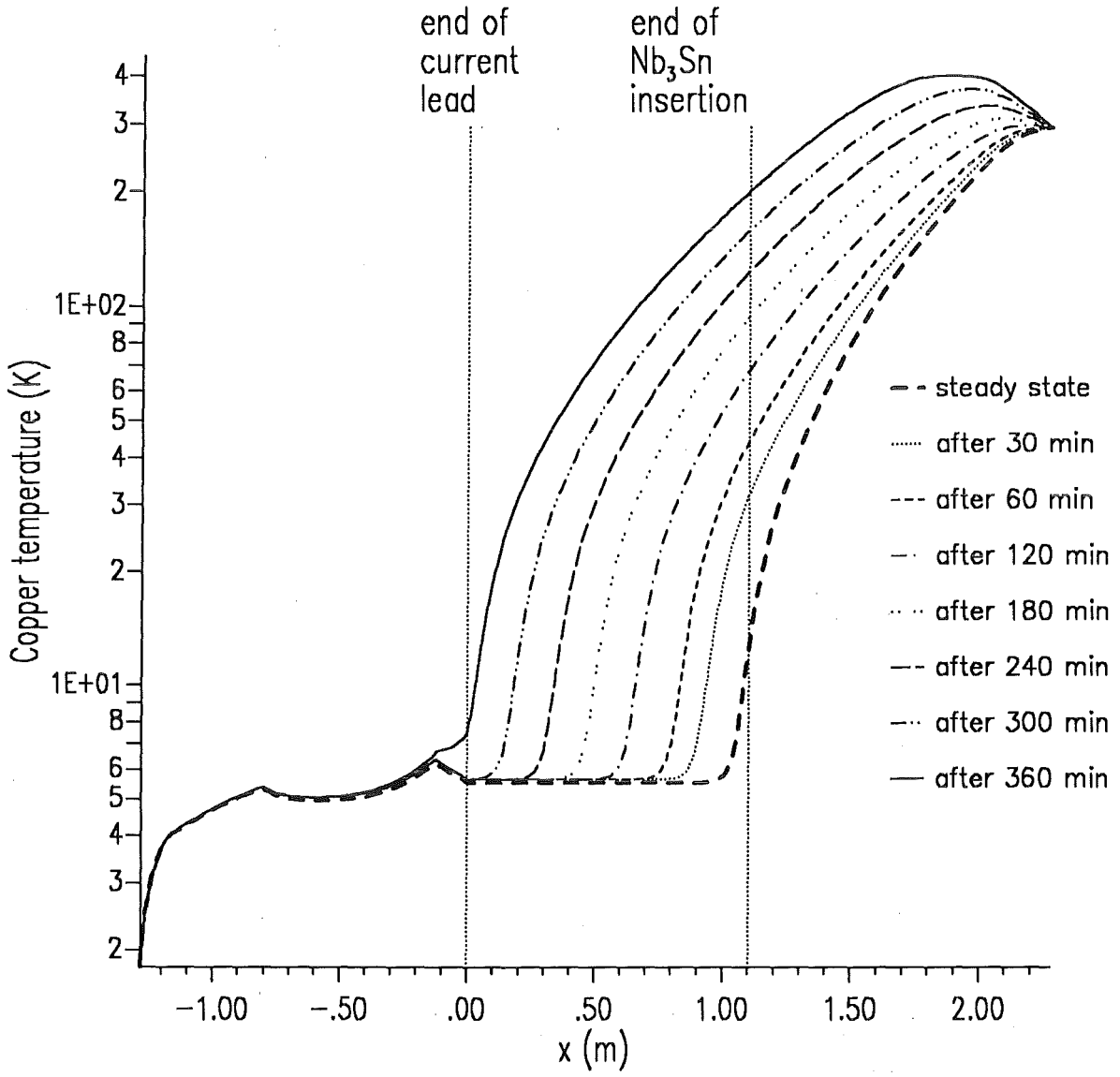

Figure 16. Temperature profile of the lead bus system for 23 kA at different times after changing the mass flow rate: The dashed line denote the steady state solution for a mass flow rate of 1.30 g/s, the different lines correspond to different times after changing the mass flow rate to 1.10 g/s

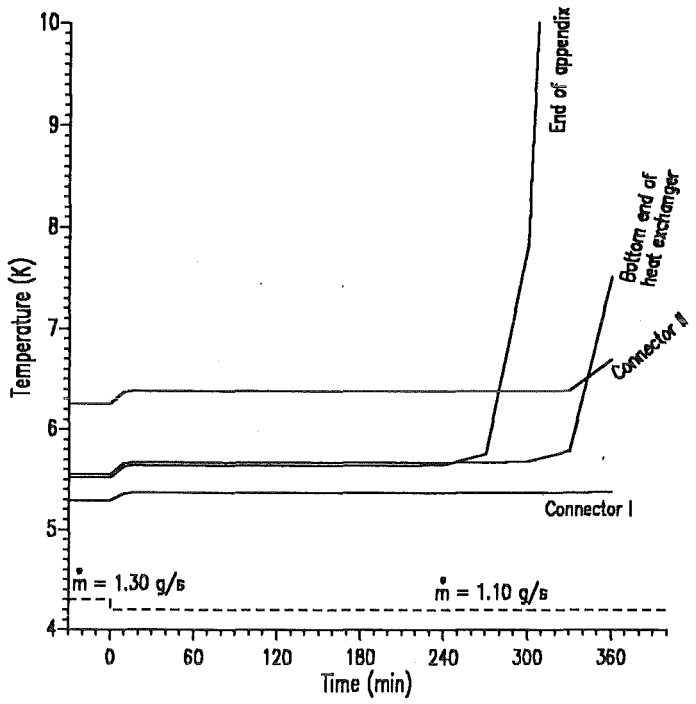

Figure 17. Different temperatures at the cold end resp. the bus bar system vs time after changing the mass flow rate: The temperature increase due to the change of the mass flow rate from 1.30 g/s to 1.10 g/s takes place immediately after this change but is only in a range of 0.08 K to 0.13 K

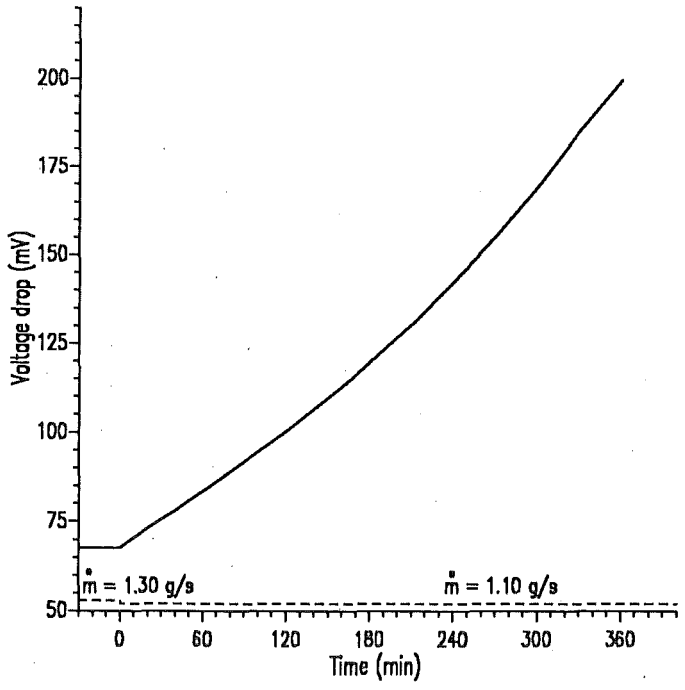

Figure 18. Voltage drop vs time after changing the mass flow rate

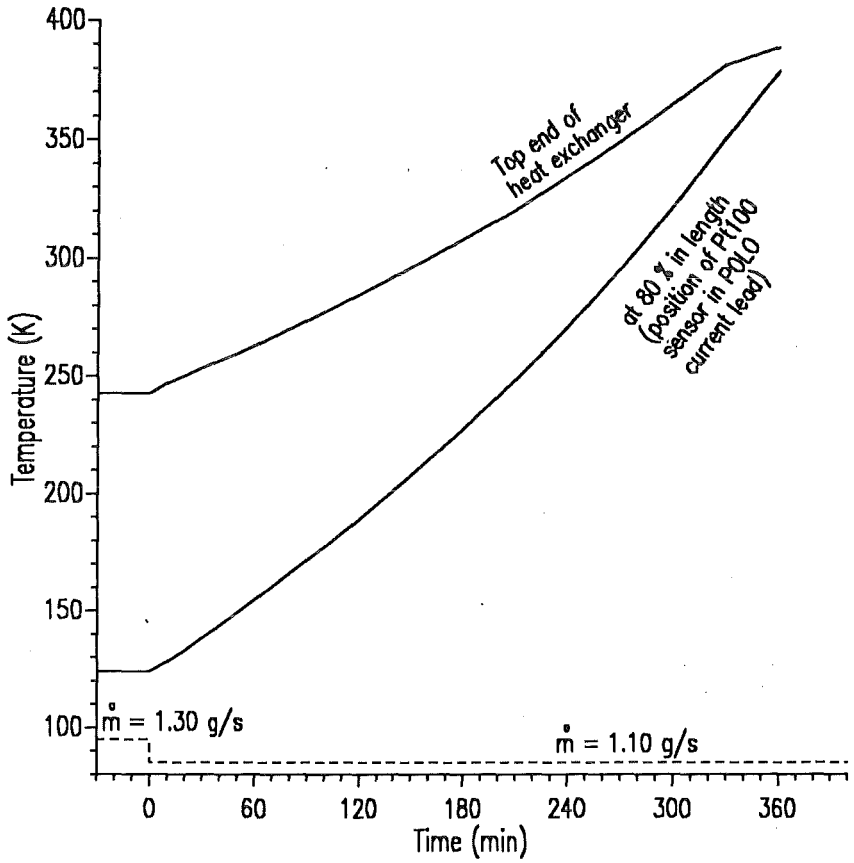

Figure 19. Copper temperatures at the top end of the heat exchanger resp. at 80 per cent position in length vs time after changing the mass flow rate

The transient behaviour is different in case of a change of mass flow to a value which is above or at the critical mass flow rate e.g. from 1.40 g/s to 1.27 g/s. In the latter case, the temperatures as well as the voltage drop converge to numbers which belong to a steady state temperature profile well optimized. This can be seen in Figure 20 where the voltage drop is plotted vs time for both transient cases i.e. diverging and converging. Diverging in this sense means that the steady state number is well above a physically stable limit.

The behaviour of the lead bus system looks different if switching the mass flow rate from 1.27 g/s to 1.40 g/s i.e. in the opposite manner than before. The corresponding voltage drop is also seen in Figure 20, as a dashed line.

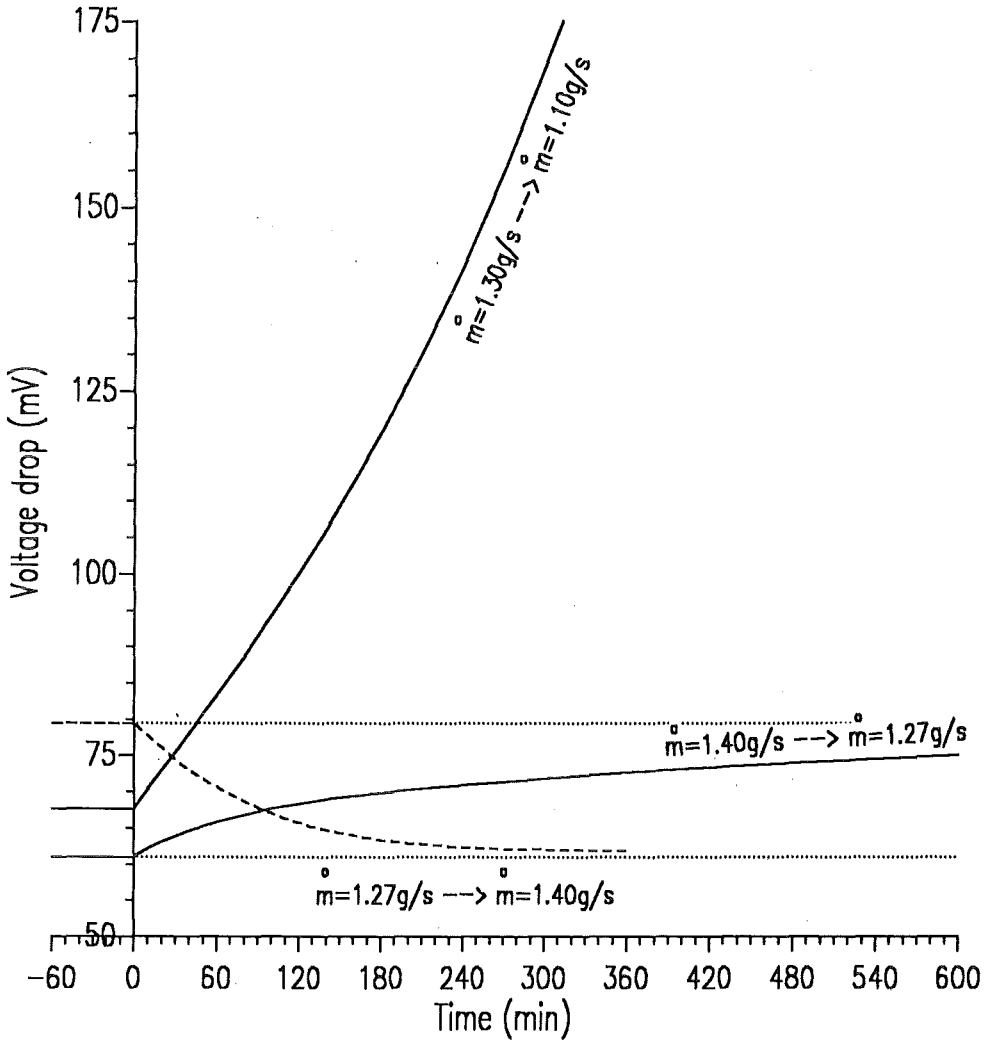

Figure 20. Voltage drop vs time after changing the mass flow rate: The diverging curve corresponds to a change of mass flow to a value which is below the critical mass flow rate as shown in Figure 12. The converging curve corresponds to a change of mass flow to a value which is the critical mass flow rate. The dashed curve belongs to a change in mass flow from a lower to a higher number

4.4.2 Change of mass flow at zero current

The same time depending behaviour has been investigated for zero current. Figure 21 shows the temperature profiles for the steady state solutions obtained for 0.38 g/s resp. 0.30 g/s. In addition, profiles are plotted resulting at different times after switching the mass flow rate from 0.38 g/s to 0.30 g/s. After one hour, the temperature profile lies in between the steady state solution started and the steady state one envisaged.

In Figure 22 the temperature at the cold end of the heat exchanger is plotted vs time. After 24 h, the temperatures are not reaching the new equilibrium state!

Thus, a permanent helium mass flow even for times without shifts and/or experiment will be recommended.

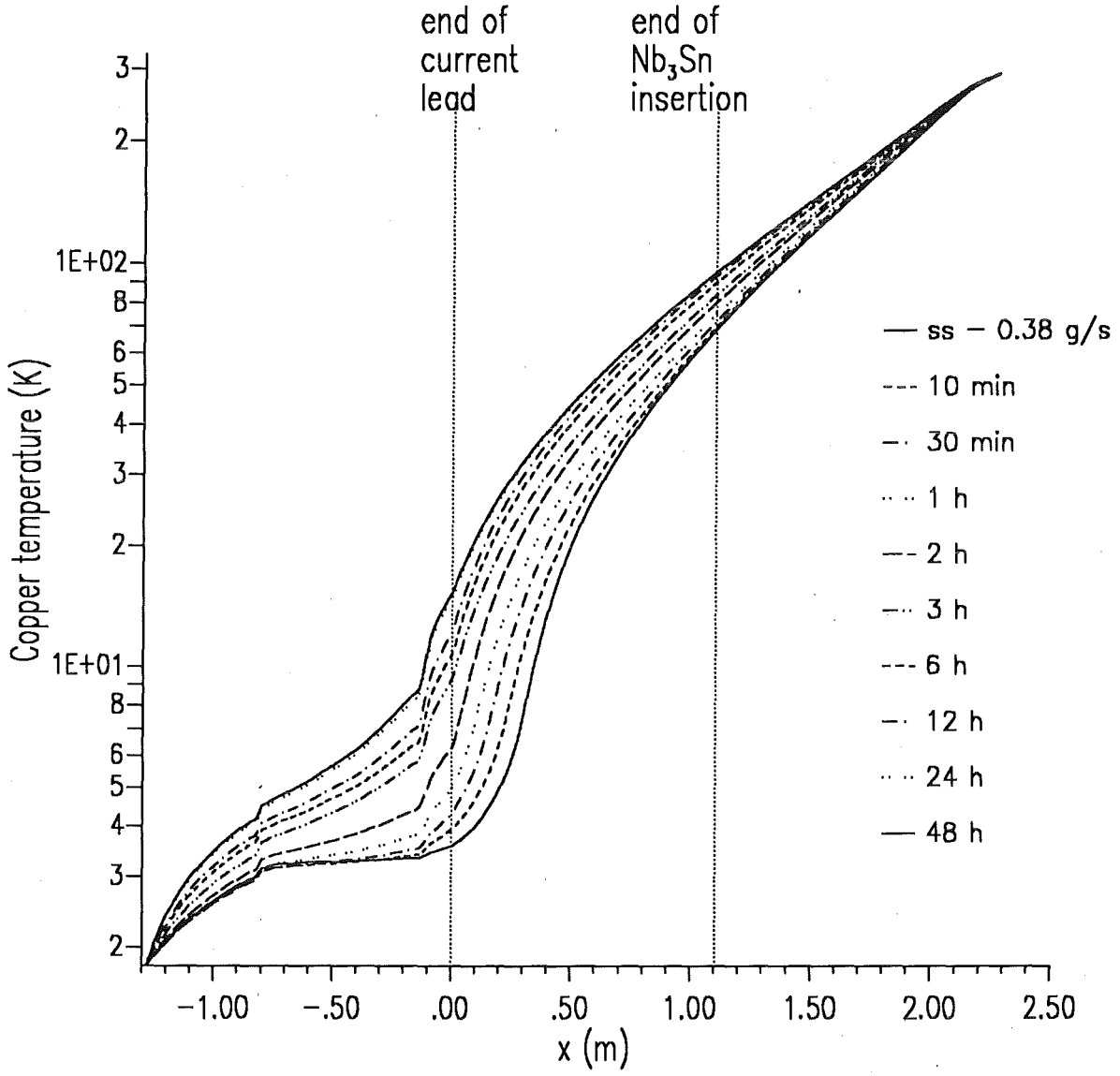

Figure 21. Temperature profile of the lead bus system for 0 kA for different times after changing the mass flow rate: The dashed line denotes the steady state (ss) solution for a mass flow rate of 0.38 g/s, the different lines correspond to different times after changing the mass flow rate to 0.30 g/s

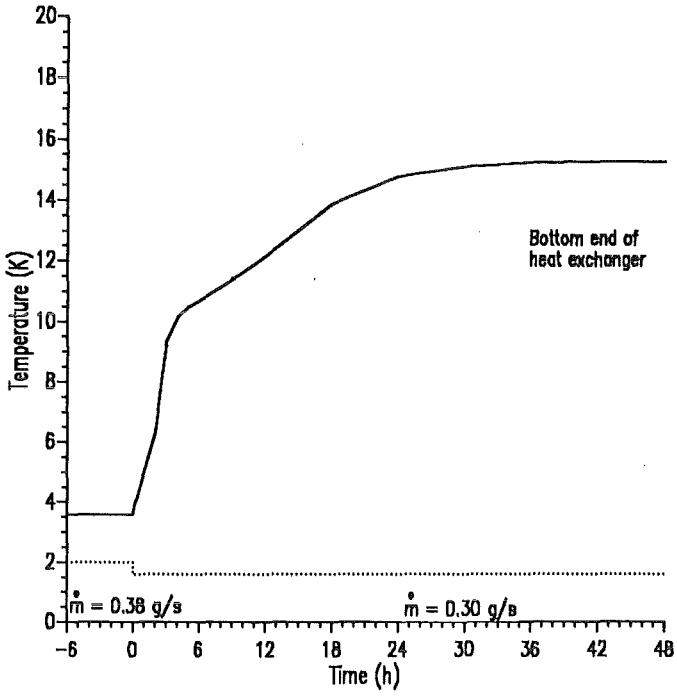

Figure 22. Temperature profile at the cold end of the heat exchanger at 23 kA for different times after changing the mass flow rate

4.4.3 Change of mass flow while switching the current from 0 to 23 kA

Finally,the time depending behaviour of the lead and bus system has been computed in case of switching on the current from zero to 23 kA, and changing the mass flow rate simultaneously from 0.38 g/s to 1.27 g/s. The resulting temperature profiles have been plotted in Figure 23. The temperature profile at the bus bar system changes relatively fast i.e. after roughly half an hour, the final profile has been reached without any overheating. The heat load towards the coil winding also changes fast to the steady state number for 23 kA. The change of the temperature profile of the current lead itself, especially the warm part of the lead, needs much more time. Moreover, the temperature reaches a higher value than the steady state one (after roughly 5 h) and falls back slowly. This can also been concluded from the voltage drop behaviour as shown in Figure 23.

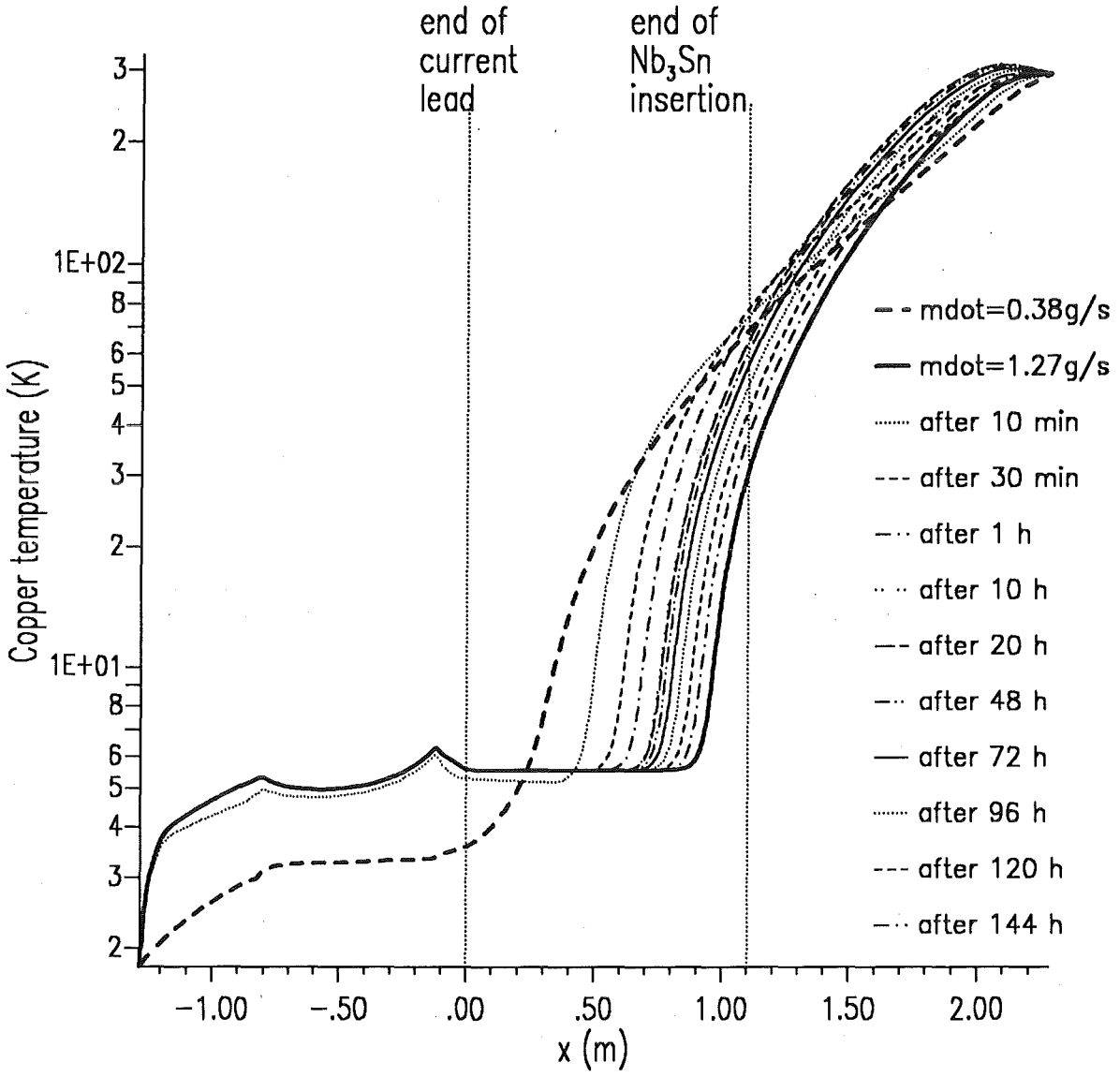

Figure 23. Temperature profile for different times after changing the mass flow rate and switching the current from 0 to 23 kA: The dashed line denotes the steady state solution for a mass flow rate of 0.38 g/s at zero current, the different lines correspond to different times after switching to 23 kA and changing the mass flow rate to 1.27 g/s

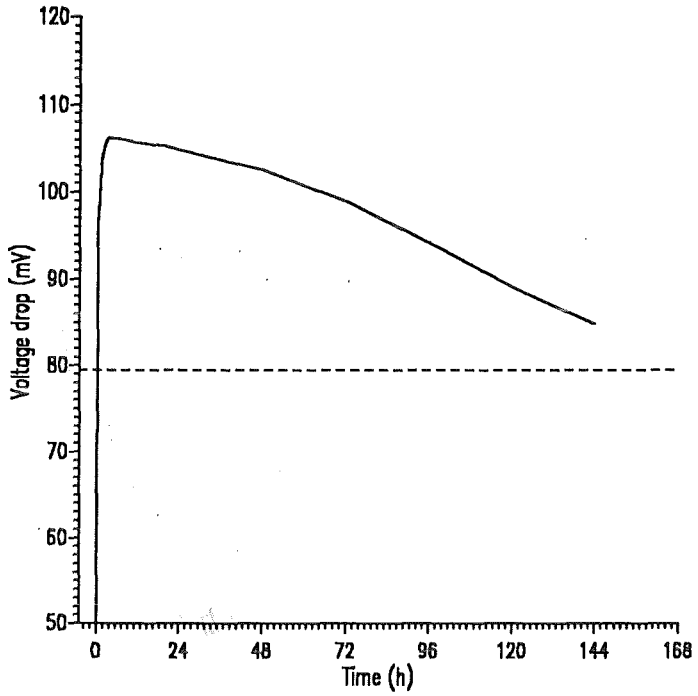

Figure 24. Voltage drop for different times after changing the mass flow rate and switching the current from 0 to 23 kA: The dashed line corresponds to the steady state value at 23 kA, 1.27 g/s

5. Eddy current losses in the superconducting bus bar during energy dump

During the fast discharge of the LCT coil, eddy currents are induced in the stabilizing copper bar of the superconducting bus. The respective losses can be calculated by using the so-called "box-formula" given in [7] although experiments with the LCT coil have shown that the measured losses are much lower than the ones computed by using this formula (see e.g. [8]). Here, the losses are given per unit volume (small letters) or length (capital letters).

$$p_{E,t} = \frac{n_p \tau}{\mu_0} \dot{B}_t^2 \quad [W/m^3]$$

or

$$P_{E,t} = p_{E,t} A_{bus} \quad [W/m]$$

$$q_{E,t} = \frac{n_p \tau}{\mu_0} \int \dot{B}_t^2 dt \quad [J/m^3]$$

or

$$Q_{E,t} = q_{E,t} A_{bus} \quad [J/m]$$

where
n_p = number of stages,
τ = time constant,
A_{bus} = cross section of the s.c. bus,
$\mu_0 = 4\pi\ 10^{-7}$ Vs/Am.

The time constant is defined as follows.

$$n_p \tau = \frac{1}{12} \mu_0 \frac{a^3 b - c^3 d}{ab - cd} \frac{1}{\rho}$$

where in addition
a, b = outer length of the copper box of the s.c. bus,
c, d = inner length of the copper box of the s.c. bus,
ρ = resistivity of the copper.

The losses due to the parallel field change will be neglected because the respective component is only a few percent of the transversal one.

The calculation of the losses requires the knowledge of the transient field changes i.e. $\dot{B}$ resp. $\dot{B}^2$ at the area of the position of the superconducting bus bar. Therefore, the magnetic fields have been calculated starting from a coil current of 21 kA for a dump time constant of 15 s at different times and corresponding currents up to 40 s by means of the computer code EFFI [9]. From these field values, the difference-quotients $\Delta B/\Delta t$ resp. $(\Delta B/\Delta t)^2$ are calculated and from this the quantities needed for the evaluation of the losses are deduced i.e.

$$\left[\frac{\Delta B}{\Delta t}\right]^2_{max}$$

$$\int_0^{40s} \left[\frac{\Delta B}{\Delta t}\right]^2 dt$$

The resultant numbers are as follows:

$$\left[\frac{\Delta B}{\Delta t}\right]^2_{max} = 0.0047\ T^2/s^2 \quad \text{(after 1 s)}$$

$$\int_0^{40s} \left[\frac{\Delta B}{\Delta t} \right]^2 dt = 0.0143\, T^2/s$$

Using the geometrical numbers given in Table 2, i.e. a = b = 50 mm, c = 7.2 mm d = 38.4 mm, $\rho = 2\ 10^{-10}\Omega m$, the time constant is computed to $n_p\tau = 1.468$ s. From this, the maximum power resp. average energy losses are calculated resulting in the following numbers

$$p_{E,t} = 5492\, W/m^3$$

or

$$P_{E,t} = 12.2\, W/m$$

resp.

$$q_{E,t} = 1.67\ 10^4\, J/m^3$$

or

$$Q_{E,t} = 37.2\, J/m$$

These numbers are used in the following to compute the so-called "hot spot temperature" i.e. the maximum temperature in a superconductor reached due to power dissipation.

6. Hot spot temperature in the superconducting bus bar during energy dump

The maximum temperature in the superconducting bus bar has been calculated by using the energy input per unit length deposited in the s.c. bus due to eddy currents produced during a fast discharge of the LCT coil.

The calculations were done by means of the computer code HOTSPOT written by L. Bottura [10]. To indicate the effect of loss of mass flow, the hot spot temperature was computed once with and once without the availability of the helium enthalpy. Also, the capacity of the stabilizing copper part of the s.c. bus was tested by assuming the absence of the superconductor as well as the helium.

The results of the computations are shown in Figure 25. There, the temperature of the s.c. bus is plotted vs time during coil dump for the three cases mentioned above. The coil current is also shown.

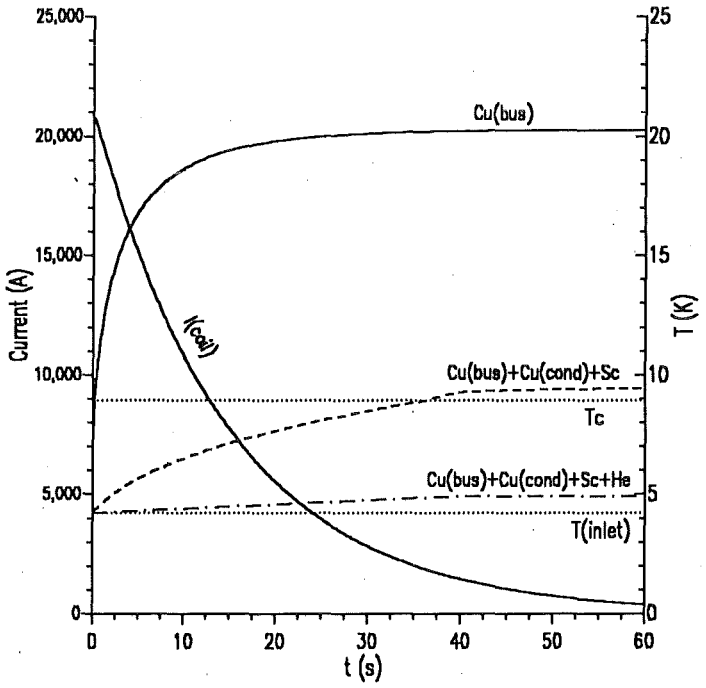

Figure 25. Hot spot temperature of the superconducting bus vs time: The full line denotes the fact that only the enthalpy of the stabilizing copper of the bus has been used, for the dashed line the enthalpies of the superconductor resp. the copper content of the conductor has been used, too. For the dash-dotted line the enthalpy of the helium has been additionally used. The energy dump has been shown, too

The maximum temperature reached in the superconducting bus bar by taking into account only the helium enthalpy is about 20 K i.e. no dangerous temperature level. If taking into account the enthalpy of the helium, the bus bar system will stay in its superconducting state during current dump.

It should be mentioned that the physical model used for the calculations is adiabatic i.e. the results are independent of the specific dump time if the average energy input is constant.

7. Summary and conclusions

The operation of the EURATOM LCT-coil with 1.8 K supercritical helium and a maximum operating current of 23 kA requires a new design of the superconducting bus bar system.

The system consists of the original LCT-coil terminal, a superconducting bus bar made out of a short length of the LCT superconductor imbedded in a stabilizing copper bar, and the 23 kA current lead which has been developed for the POLO project. The connections between the three parts are done by clamping. The whole connection area will be cooled by supercritical helium at 4.2 K and 4 bar which will be warmed up to room temperature by flowing through the current lead heat exchanger.

The connectors are designed for an electrical resistance of $10^{-8}\Omega$.

Although the coil winding will be at 1.8 K whereas the current lead and bus bar system will be at 4.2 K, the LCT-coil terminal need not to be cooled actively because the heat load towards the winding pack is mainly determined by the thermal conductivity due to the temperature gradient and can not be reduced by additional cooling. Therefore, the coil terminal has been kept unchanged. The heat load has been computed to be in the range of 10 - 15 W.

The optimum mass flow rate for the current lead bus system has been calculated as a function of the operating current. It results in a slightly higher number compared to calculations without superconducting bus bar due to the higher temperature at the cold end of the heat exchanger. The current lead and bus system should be able to carry currents up to 30 kA i.e. much larger than needed for the 1.8 K test of the LCT-coil.

Special attention has been given to the safety behaviour of the current lead and bus system in case of the loss of helium mass flow while the coil winding will stay cooled. The calculations show that the bus bar system is able to withstand a loss of mass flow for more than one minute without any increase of the heat load towards the coil winding even with full current of 23 kA. In case of the dump of the LCT-coil, the eddy currents induced in the copper stabilizer of the bus bar are computed, and the so-called hot spot temperature has been calculated to be below the current sharing temperature of the NbTi superconductor. Even by neglecting the enthalpy of the stagnant helium, the maximum temperature of the copper bar reaches only the 20 K level.

The quench detection of the superconducting bus system may be a problem because of its low length resp. large cross section. The total electrical resistance is roughly a factor of six larger than the sum of the two transition resistances. At 10 K, the voltage drop along the superconducting bus for 23 kA is about 2.8 mV compared to the voltage drop across the two transistion resistances of 0.23 mV each.

The current lead and bus bar system looks to be really safe.

Finally, some calculations have been done for the transient behaviour of the current lead and bus system in case of mass flow changes and the resulting question of automatic mass flow control. The calculations show that the temperature sensors at the cold end of the heat exchanger are not sensitive enough to react on small mass flow changes whereas the temperature sensors at the warm end region are better quantities. The time constant of the current lead and bus system is very large resulting in a long time needed for reaching the equilibrium state. For the operation of the LCT-coil, it is not necessary to wait for this equilibrium state, as calculations have been shown because a change of the operating current from 0 to 23 kA, and a consecutive change of the helium mass flow rate from 0.38 g/s to 1.27 g/s leads to an increase of the heat load from the bus bar system to the coil winding to the steady state value within 20 - 30 minutes. During this time, no overheating at the cold region has been found, and after this time, the temperature profile only changes in the warm region of the current lead with a very large time constant. The maximum temperature rises to about 310 K after five hours and then drops back very slowly. No dangerous overheating takes place during the time considered.

The results of all these calculations will be verified by experiment. It is planned to test the current leads at the end of 1991.

8. Acknowledgement

This work has been performed within the frame of the European Fusion Technology Programme.

9. References

[1] A. Hofmann, P. Komarek, A. Maurer, W. Maurer, G. Ries, B. Rzezonka, H. Salzburger, Ch. Schnapper, A. Ulbricht, G. Zahn, "Further use of the EURATOM LCT coil", Proc. of the 15th SOFT, Fusion Technology 1988, Elsevier Science Publishers B.V., (1989), 1596

[2] A. Grünhagen, R. Heil, R. Heller, W. Herz, A. Hofmann, K. Jentzsch, H. Kapulla, H. Katheder, B. Kneifel, P. Komarek, W. Lehmann, W. Maurer, H. Müller, H. Pulch, W. Reeb, G. Schenk, F. Spath, M. Süßer, A. Ulbricht, G. Zahn, "Preparations of the TOSKA facility at KfK for testing of NET model coils", Proc. of the 16th SOFT, Fusion Technology 1990, Elsevier Science Publishers B.V., (1991), 1692

[3] S. Förster, G. Friesinger, R. Heller, U. Jeske, G. Schenk, G. Nöther, C. Schmidt, L. Siewerdt, M. Süßer, A. Ulbricht, F. Wüchner, P. Bonnet, A. Bourquard, F. Geyer, H. Schadt, "Development of components for poloidal field coils within the KfK POLO project", Proc. of the 16th SOFT, Fusion Technology 1990, Elsevier Science Publishers B.V., (1991), 1706

[4] R. Heller, "Numerical calculation of current leads for fusion magnets", KfK 4608, (1989)

[5] R. Heller and U. Jeske, Oktober 1989, unpublished report

[6] SIEMENS, "Supraleitender Torusfeldmagnet, LCT-EURATOM, Large Coil Task", KfK Auftrag 130/D1/427.841, Endgültiger Entwurf, Abschlußbericht 03/84, Band A: Entwurf, Versuche, Planung, unpublished

[7] K. Kwasnitza et al., " Basic equations for the calculation of AC losses in the conductor for the superconducting NET-TF coils", KRYO-86-13, October 1986

[8] D.S. Beard, W. Klose, S. Shimamoto and G. Vécsey (eds.) "The IEA Large Coil Task. Development of Superconducting Toroidal Field Magnets for Fusion Power", Fusion Engineering and Design, 7 (1 & 2), (1988), pp 1 - 232

[9] S.J. Sackett, "EFFI, a code for calculating the electromagnetic field, force and inductance in coil systems of arbitrary geometry", LLNL, Livermore, California, UCRL-52402 (1978)

[10] L. Bottura, private communication